Explorative Spectrometric Evaluations of Frying Oil Deterioration

Søren Balling Engelsen*

The Royal Veterinary and Agricultural University, Food Technology, Department of Dairy and Food Science, Rolighedsvej 30, DK-1958 Frederiksberg C, Denmark

ABSTRACT: The potential of spectroscopy as a reliable and fast method for determining the deterioration of frying oils was investigated. Daily oil samples were collected from a commercial Chinese spring roll plant. The plant was operated one shift, 5 d a week, then cleaned and restarted with fresh oil every 4 wk. Each oil sample was analyzed by 11 chemical/physical methods and fluorescence, near infrared/visible (NIR/VIS), Fourier transform infrared (FT-IR) and FT-Raman spectroscopic procedures. The results were evaluated and compared by principal-component analysis and partial least squares regression. Most chemical/physical and all spectroscopic methods detected the deterioration during the first half of the frying cycle. Thereafter, an equilibrium occurred between deterioration processes and replenishment with new oil. At equilibrium, the correlation between frying time and the various methods was nonlinear. FT-IR with the attenuated total reflectance sampling technique was the most direct and accurate method of monitoring gross changes in the frying oil. Fluorescence was the technique that provided the best models for anisidine value, oligomers, iodine value, and vitamin E. NIR/VIS spectroscopy proved to be a good general-purpose technique. The study demonstrated that spectroscopic sensors have the potential to replace titration and chromatographic procedures, and can be used in combination with chemometric data analysis to optimize deep-frying operations.
JAOCS 74, 1495–1508 (1997).

KEY WORDS: Chemometrics, fluorescence, frying oil, FT-IR, NIR, Raman, VIS.

During deep-fat frying, the oil undergoes a series of complex chemical reactions, such as oxidation, polymerization, hydrolysis, *cis*/*trans* isomerization, conjugation, pyrolysis, and cyclization (1,2). These reactions are known to affect organoleptic, nutritive, and functional properties of the fried food and, in the long run, can result in the formation of compounds that have adverse health effects (3,4). Objective analytical methods are required for accurate quality assessment of used frying fats/oils. However, it has not yet been possible to find an easy, reliable, practical analytical solution to predict when to discard the oil (2,4–6). Difficulty in finding an objective analytical procedure is due partly to the complexity of compounds formed in the frying oil and partly to the lack of generally accepted nutritional and toxicological minimum/maximum values. Further complications arise because any analytical chemical/physical test used will be affected by the frying oil quality (the more unsaturated the oil, the greater the tendency to form polymeric rather than polar degradation products), the food being fried, and by the replenishment with new oil necessary to maintain the oil bath (6).

*E-mail: engelsen@muscadet.mli.kvl.dk.

Spectroscopic methods, along with chemometric multivariate analysis, are emerging as potential tools for rapid screening of oil authenticity and quality (7,8), but their capabilities to monitor and detect frying oil deterioration in industrial deep-fat frying operations remain largely unexplored. Spectroscopic sensors have the advantage that the measurements are rapid and noninvasive and that they can be installed on-line/at-line. Chemometric data analysis has the advantage that it is able to deal efficiently with real-world multivariate data, including highly co-linear spectral data, which are observed rather than manipulated. Development of rapid spectroscopic methods to evaluate frying oil deterioration in the food industries is desirable, not only to assess frying oil quality but also to gain insight and to monitor the main variables that influence the frying process, i.e., quality of the frying oil, the fried food itself, frying temperature, duration of use, turnover rate, exposure to oxygen, use of antioxidants or antifoams, filtering, handling of the frying equipment, and maintenance of the frying oil. By using spectroscopic methods along with chemometric methods, the complete frying process can be monitored on-line, and changes to improve the quality and to extend the fry life of the oil can be suggested.

The present investigation aims to evaluate the potential of different spectroscopic sensors and to demonstrate the advantage of applying multivariate chemometric projection and calibration tools for monitoring the oil deterioration in a commercial frying operation. For this purpose, daily oil samples were collected from a commercial spring roll plant, investigated by a large variety of chemical/physical analytical tests, and subsequently investigated spectroscopically in a variety of spectral regions by different spectral methods.

EXPERIMENTAL PROCEDURES

Samples. Daily oil samples were collected from a commercial Chinese spring roll plant (Daloon A/S, Nyborg, Den-

mark), which operated one shift 5 d a week and was cleaned and started with fresh oil every 4 wk. Sample 1 is from new oil only heated up in the fryer; sample 2 is from the following working day and so forth. Sample 20 is from the oil that was discarded, according to the practice of the company. During nights and weekends, the oil was stored in a separate tank, allowing the oil to cool to room temperature. The deep-fat fryer batch volume was 3,000 L, and new oil was continuously added to compensate for the oil absorbed into the spring rolls (approximately 5 g per roll). The frying process took place at temperatures around 180 to 190°C, and each spring roll was deep-fried for approximately 90 s. The oil, acquired at Århus Oil Factory A/S (Århus, Denmark), consisted of a typical blend of fractionated and deodorized rapeseed oil (25%) and palm oil (75%). The ratio between saturated fatty acids, monounsaturated fatty acids, and polyunsaturated fatty acids was 29:52:19. About 16% of the polyunsaturated fatty acids was linolenic acid. The total natural content of vitamin E in the oil was about 750 μg/g.

Spectroscopic data. To resemble on-line measurements as closely as possible, all spectroscopic evaluations of the samples were performed without any pretreatment, such as dilution or filtering. All spectral measurements were made at room temperature.

Fluorescence data were collected on a Perkin-Elmer LS50B spectrometer (Palo Alto, CA). The spectra were acquired by using a quartz cuvette in a 90° arrangement. Complete excitation–emission two-dimensional landscapes were collected for the first and last oil samples to determine optimal excitation wavelengths. The excitation wavelengths 395, 420, 440, 500, and 530 nm were selected from the landscapes. Emission spectra were recorded from the excitation wavelength plus 20 nm, to avoid Rayleigh scattering, and up to 800 nm. In subsequent data treatment, the five emission spectra were appended and stored as one spectrum (Table 1).

Dispersive near-infrared (NIR/VIS) data (including the visible region) were collected with an NIRSystems Inc. (model 6500; NIR Systems Inc., Silver Spring, MD) spectrophotometer. The spectrophotometer has a split detector system with a silicon detector between 400 and 1100 nm and a lead sulfide detector from 1100 to 2500 nm. The NIR/VIS transmission spectra were recorded in a 10-mm quartz cell, and spectral data were converted to absorbance units.

TABLE 1
The Spectroscopic Data[a]

	Fluorescence	NIR/VIS	FT-IR	FT-Raman
Instrument	Dispersive	Dispersive	FT	FT
Sampling method	90° Emission	Transmission	HATR	180° Scattering
Reference	None	Quartz	ZnSe/KBr	None
X-variables	4386	1050	5901	3000
X-units	nm	nm	cm^{-1}	cm^{-1}
X-minimum	400	400	600	300
X-maximum	800	2500	6500	3300
Resolution	—	—	8	4/64
Accumulations	—	16	32	16
X-sampling	0.5	2	1	1

[a]NIR/VIS, near infrared/visible; FT-IR, Fourier transform infrared; HATR, horizontal attenuated total reflectance.

Fourier transform infrared data (FT-IR) were collected with a Perkin-Elmer System 2000 interferometer. Norton-Beer medium apodization functions were used to convolute the Fourier transform. The FT-IR data set was collected between 6500 and 600 cm^{-1} with a horizontal ATR (attenuated total reflectance) sampling station and a pyroelectric deuterated triglycine sulfate detector. Prior to each measurement, the sampling station was purged with dry air for 1.5 min to keep water vapor and carbon dioxide concentrations in the light path constant. For these mid-infrared measurements, the interferometer was equipped with an optimized KBr beamsplitter. All spectra were ratioed against a single-beam background spectrum, recorded with twice the number of spectral accumulations as used for the sample spectra (Table 1), and converted to absorbance units.

FT-Raman data were collected with a Perkin-Elmer System 2000 interferometer. The Raman spectra were recorded with an Nd:YAG laser emitting at 1064 nm with a laser power of 200 mW. The Raman data set was collected with an InGaAs detector and stored as Raman shifts between 3600 and 0 cm^{-1}. A 180° scattering arrangement was used, and no correction for the spectral response of the instrument was applied.

Chemical data. For each of the 20 frying oil samples, 11 different chemical/physical properties were measured (Table 2). The viscosity (VISC) of the samples was measured at 25°C with an EMILA rotational viscometer. The contents of dimeric and polymeric triglycerides (DPTG), triglycerides (TG), diglycerides (DG), monoglycerides (MG), and free fatty acids (FFA) were measured by HPSEC (high-performance size exclusion chromatography) according to the IUPAC 2508 standard (9). The mobile phase consisted of tetrahydrofuran. The HPSEC system included a pump set at a flow rate of 1.00 mL/min, three analytical columns of 300 × 7.5 mm packed with Pl-gel (500 Å + 100 Å + 100 Å), an autosampler, and a refractive index detector. DPTG was defined as all peaks, 2–3, eluted before the TG. The anisidine value (AV) was determined by the spectroscopic method described in the IUPAC 2504 standard with ultraviolet detection at 350 nm (9). The Oxifrit Test (OT) redox indicator distributed by Merck (Darmstadt, Germany) was carried out according to the accompanying instructions. The four standard categories: good, still good, replace, and bad were given values from 1 to 4, and half intervals were used when the color reading was ambiguous (Table 2). The peroxide value (PV) was determined with the titration procedure described in AOCS recommended practice Cd 8-53 (10). The iodine value (IV) was determined as described in AOCS recommended practice Cd 1b-87 (10). Finally, the total vitamin E content (vita-E) of the oil samples was determined according to the high-performance liquid chromatography (HPLC) procedure described by Podda *et al*. (11). Mobile (isocratic) phases were A: ethanol, and B: 80% ethanol + 20% water. The HPLC system included a pump set at a flow rate of 1.7 mL/min, a 250 × 4.6

TABLE 2
The Chemical/Physical Reference Data[a]

	VISC	DPTG	TG	DG	MG	FFA	AV	OT	PV	IV	Vita-E
							IUPAC 2504[c]				
Standard	Rotational viscosimeter	IUPAC 2508 HPSEC[b]					(350 nm)	Merck[d]	AOCS Cd 8-53[e]	AOCS Cd 1b-87[e]	HPLC[f] (292 nm)
Relative error	1.2%			0.8%			4–6%				5%
Unit	cps	%	%	%	%	%	—	—	meq/kg	cg I/g	µg/g
Minimum	63	0.77	62.20	5.16	0.22	0.44	12.60	1.0	0.40	33	413
Maximum	85	8.22	93.37	30.41	1.53	6.93	27.90	2.5	1.12	73	733
Average	73.45	5.92	73.88	15.51	0.90	4.29	18.64	1.6	0.88	53.55	506
SD	5.92	2.29	11.01	6.73	0.51	2.39	4.37	0.6	0.23	13.10	98

[a]VISC, viscosity; DPTG, dimeric and polymeric triglycerides; TG, triglycerides; DG, diglycerides; MG, monoglycerides; FFA, free fatty acids; AV, anisidine value; OT, Oxifrit Test; PV, peroxide value; IV, iodine value; vita-E, vitamin E.
[b]HPSEC, high-performance size exclusion chromatography; IUPAC 2508 (Ref. 9).
[c]IUPAC 2504 (Ref. 9).
[d]Darmstadt, Germany.
[e]AOCS Cd 8-53 (Ref. 10); AOCS Cd 1b-87 (Ref. 10).
[f]HPLC, high-performance liquid chromatography.

mm, 5-µm particle diameter. Chromspher C18 stainless-steel column (Chrompack Int., Raritan, NJ), an autosampler, and a fluorescence detector. Detection was set at excitation 292 nm, and emission at 325 nm. Six peaks were detected for α-tocotrienol, β-tocotrienol, γ-tocotrienol, α-tocopherol, β-tocopherol, and γ-tocopherol, respectively. In the quantitation, integration of the peaks was related to tocopherol standards. Determination of tocotrienolic content was based on the response functions developed for the corresponding tocopherols. The vita-E content (Table 2) was determined as the sum of all six substances.

Chemometrics. Chemometrics is the science of relating measurements made on a chemical system or process to the state of the system *via* application of mathematical or statistical methods (definition by the International Chemometrics Society). One of the main advantages of chemometric methods is that they are able to deal with spectral information that contains multivariate colinear data. Chemometrics allows us to analyze the frying operation as a whole, initially with the sacrifice of understanding on a more fundamental level but with the capability of providing global information that later feeds back into low-level knowledge.

Principal component analysis (PCA) is a powerful technique for compression of large multivariate data sets, such as spectral information (12). The multidimensional data set is resolved into orthogonal components whose linear combinations approximate the original data set in a least squares sense. In PCA, the original data matrix (X) is decomposed into a score matrix (T) and a loading matrix (P), and the residuals are collected in a matrix (E):

$$X = TP^T + E \quad [1]$$

Only a limited number of principal components (PC), equal to the chemical rank of the X-matrix, are relevant in describing the systematic information in X. The loading vectors for the PC can be considered as pure hidden spectra that are common to all measured spectra. What makes the individual raw spectra different are the amounts (scores) of hidden spectra. The scores contain information about samples and the loadings about the variables (13).

Partial least squares (PLS) regression is a predictive two-block regression method based on estimated latent variables and applies to the simultaneous analysis of two data sets (e.g., spectra and physical/chemical tests) on the same objects (e.g., frying oils) (14). The purpose of PLS regression is to build a linear model that enables prediction of a desired characteristic (y) from a measured spectrum (x). In matrix notation, we have the linear model $y = Xb$ where b contains the regression coefficients that are determined during the calibration step. PLS was first applied to NIR spectra by Martens and Jensen in 1983 (15) and is now used routinely to correlate spectroscopic data (rapid measurements) with related chemical/physical data (slow chemical/physical measurements).

Principal variables is a method for selecting a limited number of original variables (wavelengths) that describe as much as possible of the variance in the data matrix (spectra) or, alternatively, in a vector with a desired characteristic (chemical/physical measurement) (16). Besides being important when developing robust PLS models and when optimizing filter instruments, principal variables selection is also helpful in interpretation of the models (13). The principal variable method is initiated by finding the variable (wavelength) that covaries most with the y-vector (physical/chemical measurement). This variable is the first principal variable. The original data matrix is then reduced (orthogonalized) with respect to the first principal variable. Then new covariant variables in the reduced data matrix are selected iteratively. The result of the principal variable selection is a limited number of the original variables (e.g., wavelengths), while PCA/PLS selects latent factors based on information from all original variables (vectors). If the objective is to build predictive models, it is subsequently necessary to apply MLR (multiple linear regression) or PLS to the reduced matrix of principal variables.

Calibration/validation. Owing to the limited material available in this study (20 samples), it was appropriate to use "leave one out" (full cross) validation (17) in all evaluations reported in this study. Because of a relatively nonuniform dis-

tribution of the samples in most calibrations developed in this study, it can be argued that the equilibrium region (last 2 wk) with small sample variation should be diluted (down-scaled) in the calibration procedures. However, this approach did not lead to different conclusions.

Programs. All collected spectral data were converted to ASCII format and imported to dedicated chemometric programs. Chemometric calculations were performed with Matlab ver. 4.2c1 (The MathWorks Inc., Natick, MA) installed with PLS Toolbox ver. 1.5 (Wise & Gallagher; Eigenvector Technologies, Manson, WA) and Unscrambler ver. 6.1 (CAMO ASA, Trondheim, Norway).

RESULTS AND DISCUSSION

Chemical/physical data. The results of the tests are shown in Table 2 and are discussed and compared to national regulations collected from the literature (5,18). The impact of fat degradation on the viscosity is extremely complex and chiefly understood on a schematic level: Polymerization will increase viscosity, and decreased level of unsaturation leads to an increase in viscosity. In this study, the viscosity continued to increase through the first 11 samples, but thereafter the variation in viscosity became more randomized (Table 2). One country, Belgium, has a law that designates a maximum value (27 mPa-s at 50°C) for oil viscosity (5,18).

The presence of heat accelerates the formation of dimers and cyclic compounds through polymerization. The compounds that result from this process are large molecules formed by carbon-to-carbon and/or carbon-to-oxygen-to-carbon bridges among several fatty acids (19). Marked increases in such oligomer compounds contribute to increases in fat viscosity, foaming, and color darkening (20). In this study, the DPTG content (Table 2) continued to increase through the first 10 to 12 samples. Thereafter, the DPTG content stabilized at a level around 8%. In Belgium, the use of frying oils with more than 10% DPTG is forbidden by law; in The Netherlands, the corresponding limit is 16% (5,18).

Interestingly, no initiative has been taken to regulate the use of frying oil on the basis of diminished content of TG, DG or MG, but because the "popular" total polar content (TPC) determination (21,22) is defined as the sum of materials that are not TG, TG determination is, in principle, directly correlated to the TPC determination *via* the 100% sum. However, because the TG measurement in this study is based on separation by molar weight, oxidized TG (approximately 1 to 3%) are accounted for differently than by TPC measurement. The TG content (Table 2) decreased continuously in the first 13 samples, but thereafter it stabilized at a level around 65%—a value which is slightly lower than the generally accepted limits for a degrading frying oil, *viz*., TG below 75% and TPC above 25% (23–25).

Determination of FFA appears to be a favored method for internal quality control evaluation of frying fats in the food industry. FFA are formed by oxidation as well as by hydrolysis, and unfortunately the tests used for FFA determination cannot distinguish between FFA formed by hydrolysis and those formed by oxidation. Some previous studies have found a high correlation between FFA or TPC and length of frying time, suggesting that accurate prediction of oil abuse is possible (20). In this study, the FFA content (Table 2) increased through the first 13 samples to reach a level of 6.9%. Thereafter, the FFA level dropped slightly to a level just above 6%. In Belgium, the law forbids oils with FFA content above 2.5% (5,18).

Hydroperoxides from primary oxidation react to form secondary products whose aldehydic compounds are measured by the AV test. The AV test has an enhanced sensitivity to unsaturated aldehydes but does not measure the ketonic secondary products of oxidation (26). In this study, the AV level increased rapidly from 12.6 to 27.6 in the first three samples (Table 2), but thereafter it decreased slowly to stabilize after samples 9–12 at a level around 16. To our knowledge, AV has not been used for regulatory purposes.

The OT from Merck, which is sensitive to oxidized materials, is now used as a quick initial test for frying oil deterioration by food control officials in several countries, including Australia, Luxembourg, Portugal, and Sweden (5,18). In this study, the OT level remains at value 1 (good) in the first 9 samples, it changed to value 2 (still good) at sample 13, increased to value 2.5 (still good/replace) in sample 17, and remained at this level in the rest of the samples.

PV is the classical method for determination of peroxy groups present in oxidized fats and oils. Hydroperoxides are products of the primary oxidation in a frying oil. The PV method is based on the liberation of iodine by the hydroperoxides in an acid medium. Unfortunately, PV methods are highly empirical, and there will be variation between laboratories due to the interference of oxygen, reaction time, temperature, etc. Peroxides tend to decompose during heating and frying at 180°C (27). PV of the frying oils in this study ranged between 0.4 and 1.12 meq/kg with no significant trend (Table 2). In Australia, frying fats must have a PV less than 2 meq/kg (18).

IV is a measure of the total number of double bonds in the frying oil and thus monitors the loss of unsaturation. IV values of the frying oils in this study display a decreasing trend for the first 15 samples (from approximately 73 to approximately 38); thereafter the level stabilizes. In Finland, guidelines recommend that the frying oil must be changed if the IV has decreased by more than 16 (18).

Loss of antioxidants, such as vitamin E, from heated oils may be attributed to volatilization of the antioxidant through evaporation, decomposition, and scavenging reactions of the antioxidants (26). The natural content of antioxidant vitamin E protects to some extent the fats from oxidation by combining with radicals and stopping the chain reaction by which the free radicals multiply. In this process, vitamin E is oxidized especially by hydroperoxides, which are oxidation products of unsaturated fatty acids. In this study, the vita-E content decreased from approximately 733 µg/g to a level of approximately 430 µg/g through the first 12 samples. Several countries, including France, Norway and Switzerland, have spe-

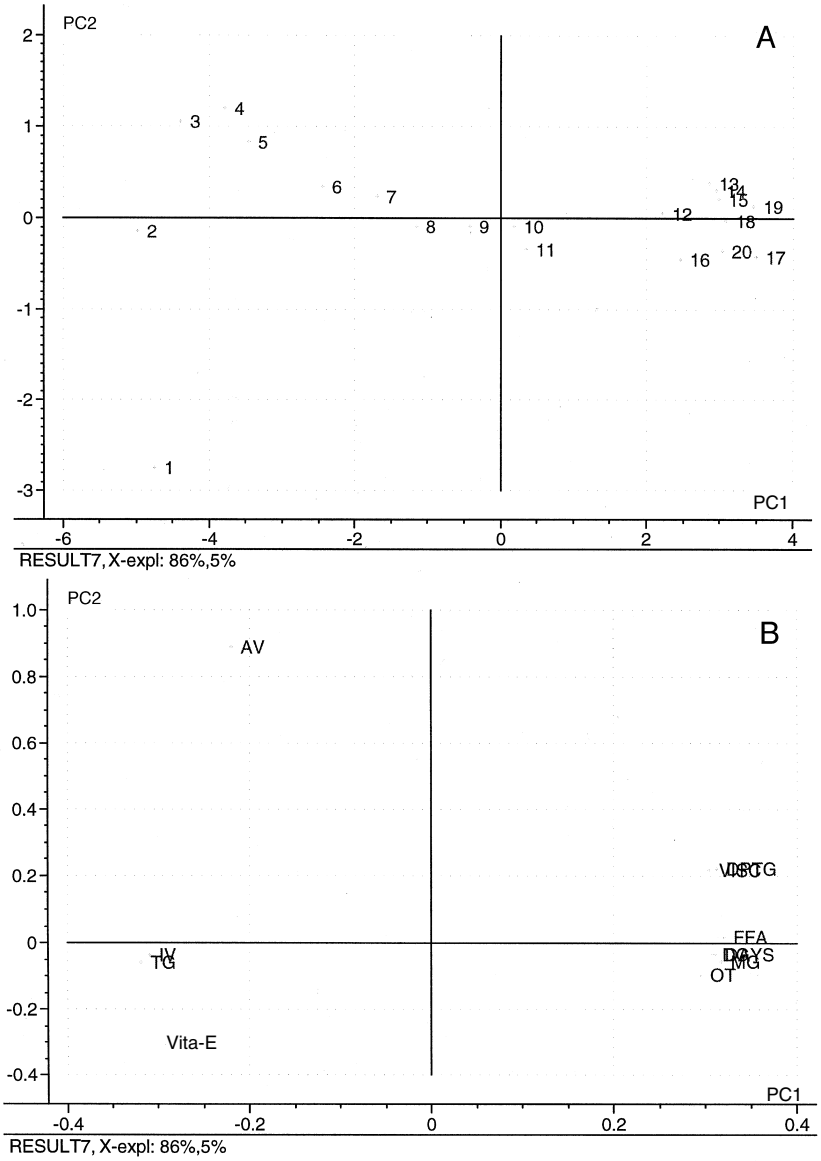

FIG. 1. (A) Score plot from principal component analysis (PCA) on chemical data measured on the frying oil samples. (B) Loading plot (*X*-loadings) from PCA on chemical data measured on the oil samples. AV, anisidine value; TG, triglycerides; IV, iodine value; Vita-E, vitamin E; OT, Oxifrit Test; MG, monoglycerides; FFA, free fatty acids; VISC, viscosity; DPTG, dimeric and polymeric triglycerides; DG, diglycerides; DAYS, time of use.

cific laws that prohibit the use of synthetic antioxidants and silicone in frying oils (18).

To investigate the internal variance structure in the chemical/physical data, a PCA was performed on the autoscaled *Y*-data. Figure 1 shows score and loading plots of the *Y*-data as a function of the two first PC. In this case, the first two PC describe 91% (86% + 5%) of the total variance in the *Y*-matrix. The fact that the three first PC describe 96% (86% + 5% + 5%) of the variance implies a high degree of redundant information in the different chemical/physical tests. The loading plot in Figure 1B shows that practically all chemical/physical tests, except AV and vita-E, are well described by the first PC. Furthermore, it shows that IV and TG are negatively correlated (decrease) to the time of use (DAYS), whereas DPTG, VISC, DG, MG, FFA, and OT are positively correlated (increase) to DAYS. Finally, vita-E was negatively correlated to AV in the second component, i.e., when the number of secondary oxidation products increased, the content of antioxidants decreased. When the score plot, Figure 1A, was compared with the loading plot (superimposed), it showed that unused but heated sample 1 had the highest content of vita-E and lowest AV and that samples 3 and 4 had maximum AV values.

To further investigate intercorrelations among the chemical/physical data, principal variable analysis of the *Y*-matrix was performed to find the most important variables. The two

most important principal variables were TG and AV, as also indicated by the PCA score plot in Figure 1A. The two variables together describe 91% (86% + 5%) of the total variance in the chemical/physical tests. This variation corresponds exactly (within rounding errors) to the explained variation in the two PC of the entire set of chemical/physical data (see above). While the first PC explains variation from the ester/free acid ratio, the second PC explains variation from secondary oxidation products. To investigate the dependency of the TG and AV variables upon the other variables, full cross-validated MLR models, using the two selected variables, TG and AV, for prediction of the other variables, were calculated. Strong positive correlations ($0.75 < R^2 \leq 1.00$) were found to DAYS, VISC, DPTG, DG, MG, FFA and IV, revealing that measurement of AV, combined with measurement of TG content, renders the other chemical/physical tests practically superfluous. Only OT ($R^2 = 0.55$) and vita-E ($R^2 = 0.65$) measurements were poorly correlated. Similar MLR models were calculated with DAYS as the only variable, and strong correlations ($0.75 < R^2 \leq 1.00$) were found to VISC, DPTG, TG, DG, MG, FFA, OT, and vita-E. Considering the high-correlation coefficient between DAYS and TG, it can be argued that simply counting the number of days in use, along with the measurement of AV, would be sufficient for industrial purposes. However, it has to be stressed that such correlation results are likely to depend on the frying object and the chemical composition of the frying oil. Nevertheless, the results support previous studies that show a high correlation between FFA or TPC and length of frying time (20,28).

Finally, it was attempted to build a PLS model of time in use (DAYS) from the autoscaled chemical/physical data (the *Y*-matrix). The resulting one-component PLS model has a correlation coefficient $R^2 = 0.95$ and a root mean square error of cross-validation prediction (RMSECV) = 1.80 days. This result will be used as a reference value when comparing the spectral PLS models below.

Fluorescence spectroscopy. Fluorimetry is a sensitive spectroscopic method, provided that the substance to be analyzed contains one or more fluorophores. Fluorescence has previously been applied to oil analysis, including quantitation of lipid hydroperoxides with dichlorofluorescein (29), analysis of high-molecular-weight oxidation products such as the fluorescent pigment, also called the lipofuscin or age pigments (30), and analysis of vitamin E (α-tocopherol) (31). In the present investigation, focus was on the quantitative aspects of fluorescence spectroscopy with regard to general deterioration of the frying oil.

To determine the most appropriate excitation wavelengths, a complete fluorescence landscape of each of the terminal samples (1 and 20) was recorded (Fig. 2). Interestingly, the two maps show that the initial two-component system with emission maxima at approximately 475 and 660 nm degenerates to a one-component system with an emission maximum at approximately 585 nm. Owing to the extremely complicated oil matrix, no attempt to assign the fluorophores will be made here. From the information in the two maps, the following five excitation wavelengths were selected for the fluorescence investigation of the 20 oil samples: 395, 420, 440, 500, and 530 nm. The resulting fivefold appended emission spectra, shown in Figure 3A, reveal a large shift in fluorescence intensity during the first 2 wk (the first 10 to 11 samples) as the frying oil becomes more used. The PCA score plot in Figure 3B has a characteristic horseshoe shape, which displays a clear development during the first 2 wk after which the spectral variation of the oil samples becomes stable with randomized variations. Apparently, an equilibrium between ongoing oxidation processes and the high turnover rate has occurred after sample 12. This is interesting because sample 11 corresponds to the Monday sample taken after weekend storage and indicates that storage of the used frying oil does not strongly affect the oxidation process. With more frequent sampling, such a PCA score plot would be a highly useful visual projection tool to monitor an industrial deep-fat frying operation (32). If the objective is to maintain an equilibrium in which oil deterioration is minimized and the operation can

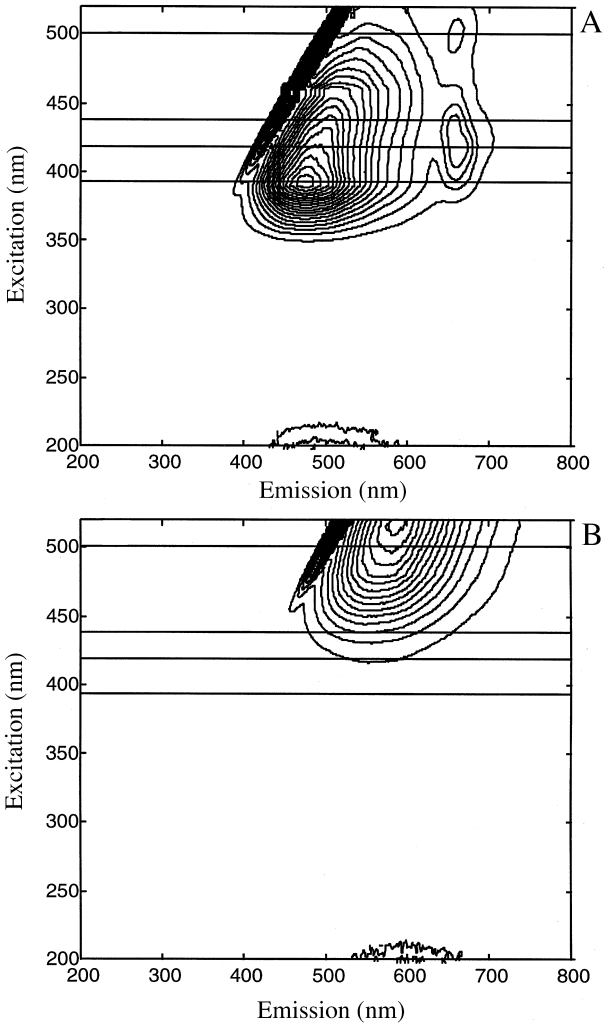

FIG. 2. Fluorescence excitation–emission landscapes. (A) Fluorescence contour mapping of sample 1. (B) Fluorescence contour mapping of sample 20. Horizontal lines indicate selected excitation wavelengths.

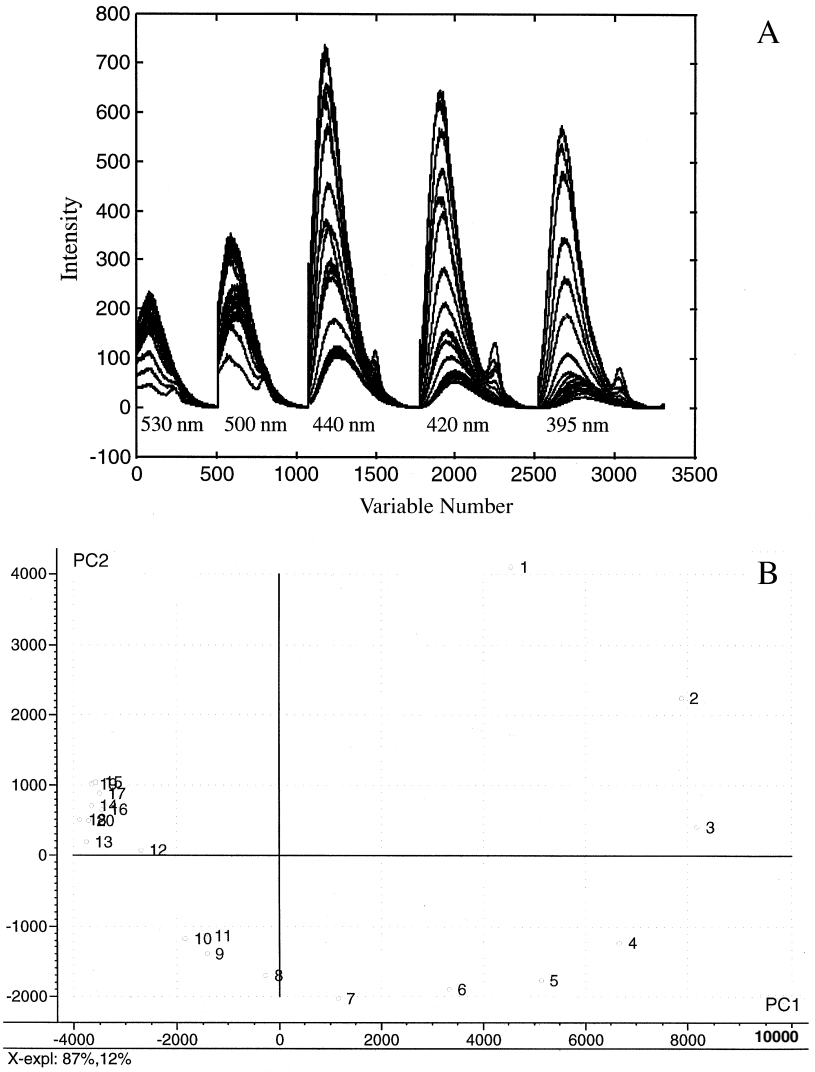

FIG. 3. (A) Appended fluorescence emission spectra of the 20 oil samples. From left to right: excitation from 530 nm, 500 nm, 440 nm, 420 nm, and 395 nm. (B) Score plot from PCA on fluorescence data as a function of the two first PC, describing 87 and 12% of the spectral variation, respectively. See Figure 1 for abbreviation.

continue indefinitely, the PCA score plot can be used to visualize any deviations from normal processing conditions and help to tune the process back in by developing appropriate response functions to process variables, such as frying temperature, filtering, antioxidant addition, and turnover rate. Ideally, this approach could be extended by relating the score plot to sensory and toxicological tests. The possible benefits could be stretching the frying life of the oil, obtaining more uniform and high quality of the frying objects and extending the shelf life of the fried objects.

From the fluorescence spectra, an attempt was made to construct quantitative PLS models to the reference chemical/physical tests. The results, listed in Table 3, show that the fluorescence spectra provide the best global correlations to DPTG, AV, IV, and vita-E determinations. In all of these but AV, the models use more than one PC, indicating the presence of important minor spectral components. Good correlations ($R^2 = 0.97$) were also found with TG, DG, MG, and FFA determinations in which the relevant compounds contain no fluorophores. Apparently, these indirect correlations arise from the fact that the ratio of oxidation and hydrolysis is constant throughout the operation. Time evolution, DAYS, can be modeled within ±1.43 d, and thus fluorescence is a more accurate predictor than the chemical/physical reference data. The existence of such a good model indicates that fluorescence spectroscopy has good potential for monitoring the overall chemical changes in the frying oil. It was not possible to build linear PLS models for the VISC and PV measurements. Because the level of PV values in the 20 samples was small (see Table 2) and the determination inaccurate, the lack of a model is not surprising. The model for AV was initially not good, but it improved significantly when the first unused sample, 1, was left out of consideration. Finally, all PLS models had better convergence behavior and slightly better per-

TABLE 3
PLS Correlations Between the Four Spectral Ensembles and Frying-Oil Quality Parameters

	DAYS	VISC	DPTG	TG	DG	MG	FFA	AV	OT	PV	IV	Vita-E
Fluorescence												
Transform[a]	log	log	log	log	log	log	log	n.t.	log	log	log	n.t.
Outliers[b]	—	—	—	—	17	—	—	1	—	—	—	—
PC (number)[c]	3	3	3	1	1	2	1	1	3	1	3	3
RMSECV[d]	1.43	2.18	0.33	1.76	0.93	0.09	0.43	1.25	0.17	0.19	3.33	22.92
$R^{2,e}$	0.94	0.86	0.98	0.97	0.97	0.97	0.97	0.91	0.92	0.24	0.93	0.94
NIR/VIS												
Transform	n.t.	n.t.	n.t.	n.t.	n.t.	n.t.	n.t.	n.t.	n.t.	n.t.	n.t.	n.t.
Outliers	—	—	—	—	17	—	—	1	—	—	—	—
PC (number)	1	3	3	2	2	1	2	1	3	1	1	3
RMSECV	1.98	1.83	0.40	1.33	0.58	0.06	0.25	1.51	0.19	0.20	4.25	23.40
R^2	0.88	0.90	0.97	0.98	0.99	0.99	0.99	0.87	0.90	0.21	0.89	0.94
FT-IR												
Transform	n.t.	n.t.	n.t.	$d/d\sigma$	n.t.	n.t.	n.t.	n.t.	n.t.	n.t.	n.t.	n.t.
Outliers	—	—	—	—	17	—	—	1	—	—	—	—
PC (number)	1	1	3	1	1	3	1	1	1	1	1	3
RMSECV	2.25	2.48	0.43	0.45	0.37	0.06	0.17	1.81	0.32	0.20	4.77	28.31
R^2	0.85	0.82	0.96	1.00	1.00	0.99	0.99	0.81	0.72	0.24	0.86	0.91
Raman												
Transform	$d/d\sigma$	log	log	log	log	log	log	log	log	$d/d\sigma$	log	log
Outliers	—	—	—	—	17	—	—	1	—	—	—	—
PC (number)	2	1	4	3	3	3	3	1	3	1	1	3
RMSECV	1.10	2.63	0.70	3.00	1.62	0.16	0.61	2.10	0.15	0.21	4.49	45.41
R^2	0.96	0.79	0.91	0.92	0.92	0.90	0.93	0.74	0.94	0.12	0.87	0.78

[a]Transformation of spectroscopic data prior to partial least squares (PLS) regression; n.t., no transformation.
[b]Sample outliers; — = no outliers. Spectra which are withdrawn from the PLS regression owing to abnormal spectrum and/or reference value.
[c]The number of principal components (PC) providing the optimal PLS fit. Owing to the limited number of samples, all models were restricted to using few PC with significant improvements in PLS performance.
[d]RMSECV = root mean square error of cross-validation.
[e]The fully cross-validated correlation coefficient R^2. When multiplied by 100, it provides the percentage of explained *y*-variance. See Tables 1 and 2 for other abbreviations.

formance when the raw intensity data were pretransformed by a logarithmic function. First- and second-derivative spectra did not improve the performance of the raw spectra.

Principal variable analysis showed that the spectral models were mainly influenced by excitation/emission wavelengths of 500/590 (emission maximum in the used frying oil), 440/540, and 395/475 nm (emission maximum in the unused frying oil). The second peak with emission maximum around 660 nm in the unused frying oil spectrum (Fig. 2), which disappeared from the oil during the first 6 to 7 d, did not influence any of the models. So, we believe that this fluorophore originates from remaining plant pigments, such as chlorophyll.

NIR/VIS spectroscopy. In the last couple of decades, with the advent of modern multivariate chemometric algorithms, NIR spectroscopy has become a powerful analytical technique. The vibrational overtone and combination bands residing in this spectral region contain an abundance of chemical information, comparable to the mid-infrared region, with the additional advantage that instrumentation is simpler and cheaper. As early as 1956, Holman and Edmondson (33) showed that absorption bands at 1690, 2150, and 2190 nm could be assigned to C–H bonds bound to *cis*-unsaturated fatty acids. More recently, Sato *et al.* (34) conducted an NIR study of spectral patterns in the NIR region of fatty acids and oils.

The NIR/VIS spectra of the 20 samples are shown in Figure 4A, and the corresponding PCA score plot in Figure 4B. The PCA score plot has a parabolic shape and, similarly to the score plot based on the fluoroscence data, the spectral variance among the first 11 samples displays a clear development. However, a large gap exists with the remaining nine samples, which again cluster in a randomly distributed equilibrium region. Whereas the fluorescence score plot shows decreasing spectral variation among the first 11 sample spectra, the NIR/VIS score plot displays the opposite tendency. This observation suggests that the variation in the two spectral ensembles is influenced by different compounds.

Table 3 lists the performance of the quantitative PLS models constructed on the basis of the NIR/VIS spectral ensemble. Owing to the extremely high reproducibility of this instrumental technique, pretransformations (scatter corrections or derivatives) of the spectra had no positive effect on the model performances. The table shows that NIR/VIS spectra provide the globally best models to VISC and MG, and that accurate NIR/VIS correlations were found for the DPTG, TG, DG, MG, and FFA measurements. As with fluorescence data, no models could be constructed for the PV measurements. The model of time evolution, DAYS, is relatively poor, presumably indicating lack of spectral information from secondary oxidation products. Because the visible spectral

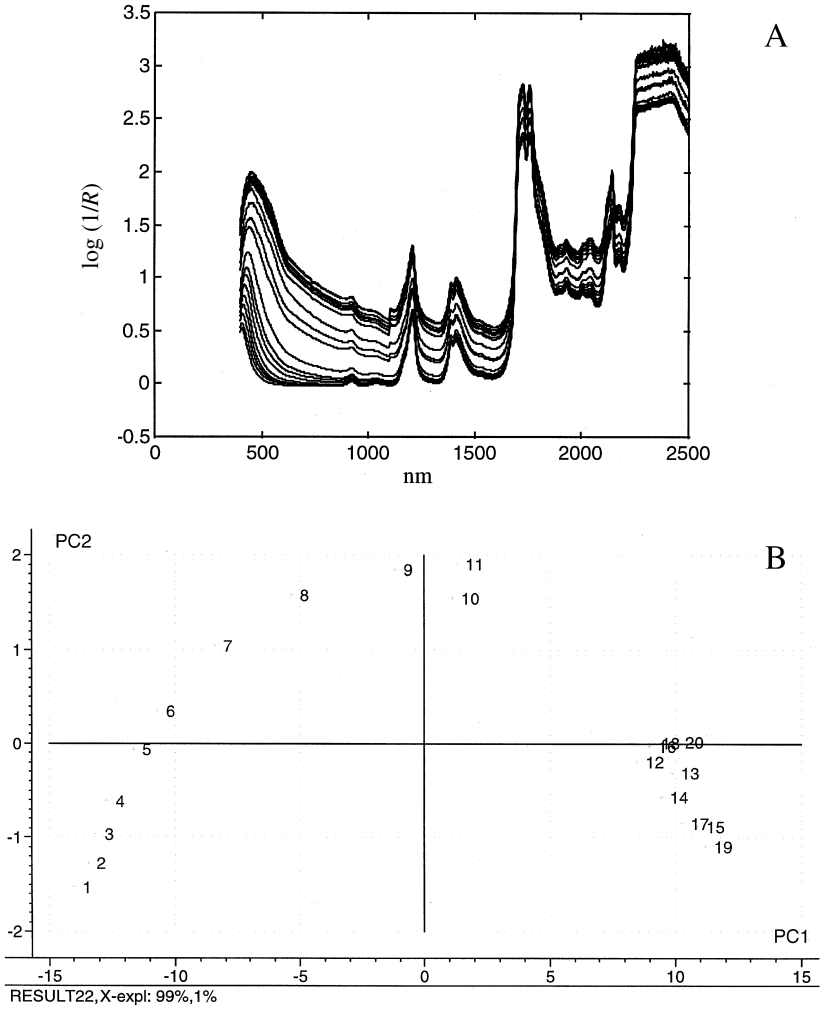

FIG. 4. (A) Near infrared/visible (NIR/VIS) spectra of the 20 oil samples. (B) Score plot from PCA on NIR/VIS data as a function of the two first PC, describing 99 and 1% of the spectral variation, respectively. See Figure 1 for other abbreviation.

region was included in the NIR/VIS measurements, we can probably also conclude that color measurements are not a good indicator of time evolution in the frying oil bath. A principle variable analysis of the best models showed that the two most influential spectral elements were 2414 and 498 nm in practically all models. The two wavelengths correspond to background scatter and a blue/green color; therefore, the models are mainly influenced by indirect correlations to the amount of dispersed material and concentration of color pigments.

FT-IR spectroscopy. The oxidation of fats and oils has been thoroughly characterized by van de Voort *et al.* (35–38) with ATR FT-IR, and precise quantitative correlations have been found for alcohol percentage, total carbonyl content, PV, FFA, IV, and saponification number (SN). In this study, however, we investigated the performance of FT-IR for monitoring the changes in the oil in a real-world frying operation rather than with a constructed sample set designed with large variations.

The superimposed FT-IR spectra of the 20 frying oil samples, shown in Figure 5A, display typical aliphatic lipid behavior. Three main peaks found in the low wavenumber region at 722, 1160, and 1460 cm^{-1} are due to polymethylene rocking deformation, C–O asymmetric ester stretching, and methylene scissoring vibrations, respectively. In the carbonyl region, we found a strong peak at 1745 cm^{-1}, corresponding to the ester C=O stretch. A closer look at this band, Figure 6, reveals a progressively increasing shoulder at about 1713 cm^{-1} corresponding to the carbonyl stretching of FFA, formed by thermal breakdown of TG into DG and MG and FFA. In the aliphatic CH stretching region, the two main peaks at 2854 and 2923 cm^{-1} correspond to symmetric and asymmetric CH stretching of the methylene groups. Finally, a weak peak at 3007 cm^{-1} corresponds to olefinic =C–H stretchings in *cis* configurations. Scrutiny of the spectra (at 966 and 1672 cm^{-1}) also reveals the presence of *trans* olefins, but they appear not to increase during the frying process. The PCA score plot in Figure 5B, based on spectral information in the FT-IR spectra, revealed that the information from the second PC was less structured than in the other spectroscopic ensembles. The

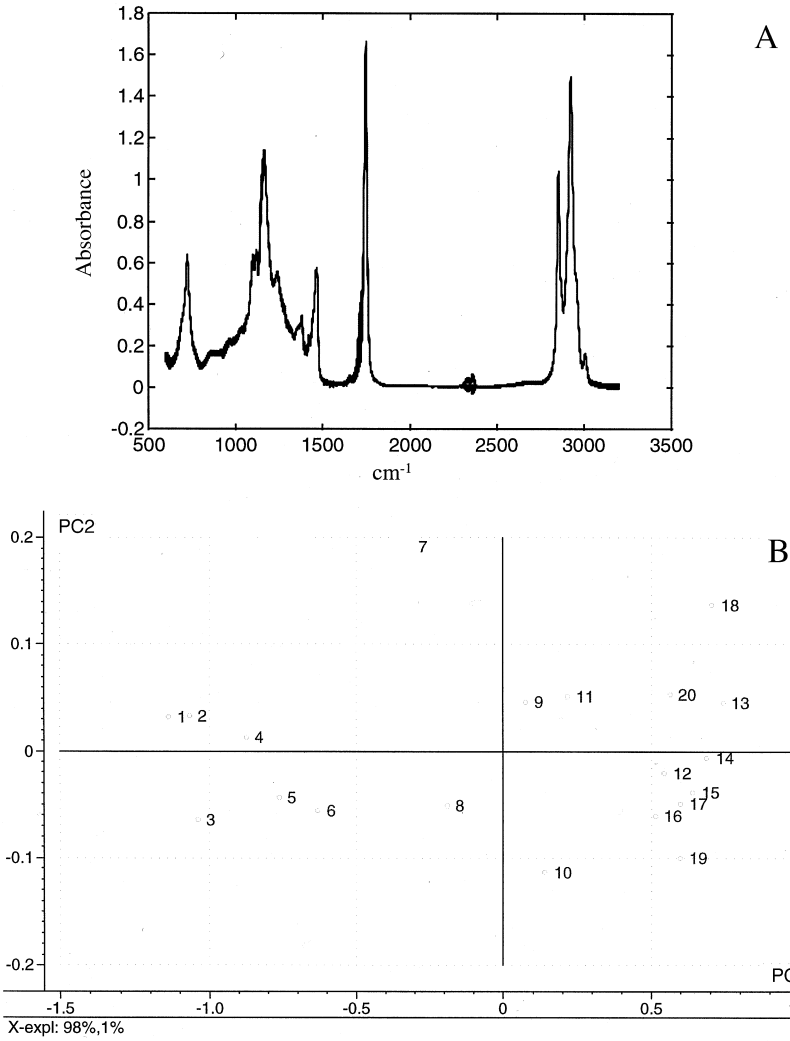

FIG. 5. (A) Fourier transform infrared (FT-IR) spectra of the 20 oil samples. (B) Score plot from PCA on FT-IR data as a function of the two first PC, describing 98 and 1% of the spectral variation, respectively. See Figure 1 for other abbreviation.

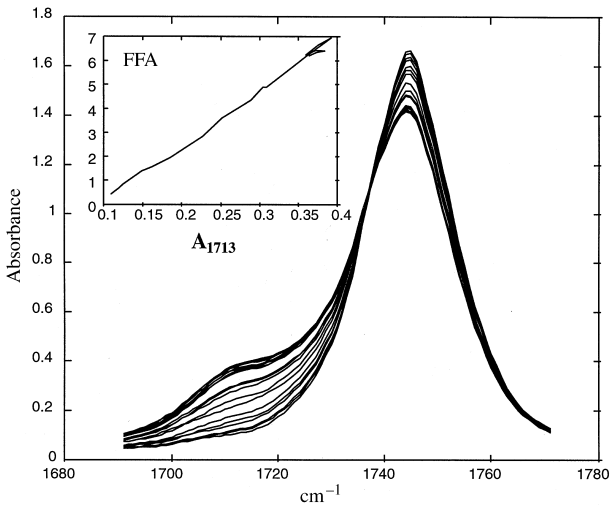

FIG. 6. The carbonyl region of the FT-IR spectra. Inserted is a graph of the linear relationship between the absorbance at 1713 cm^{-1} and the free fatty acid (FFA) determination. See Figure 5 for other abbreviation.

second PC described only about 1% of the spectral variances because almost all spectral variance was included in the first PC, i.e., 98%. When considering only the variation along the first PC, we obtained a systematic spectral variance until sample 11, from which point there is a small jump to the remaining samples with unsystematic sample variation.

The performance of PLS models to the chemical/physical data from the FT-IR spectral ensemble is summarized in Table 3. The models make use of the full-spectral information in the region from 3200 to 600 cm^{-1}, except for the region from 2600 to 1900 cm^{-1} where absorption is lacking. The table shows readily that the PLS models for TG, DG, and FFA are extraordinarily simple and accurate. These models correspond closely to the fact that, in the gross details, FT-IR spectra of the frying oil are essentially those of fatty acid esters and those of FFA. The best TG model was made from the first-derivative spectra; this pretransformation changed only the RMSECV value while the correlation coefficient of 1.0 remained unchanged. The models for DPTG and MG are also

good, presumably due to their high degree of correlation to TG and FFA. Finally, it was possible to construct a PLS model for vita-E. No good linear models could be built for DAYS, VISC, AV, OT, PV, and IV. The model for DAYS from the FT-IR data was the least satisfactory in this study, which is interesting because FT-IR is most accurate for monitoring the gross changes in the frying oil as reflected in thermal decomposition of the TG. This indicates that the apparent equilibrium that occurs after sample 11 is an equilibrium in the ratio between fatty acid esters and FFA, caused by the replenishment with new oil. If other chemical components still continue to build up, such as soluble substances from the frying objects or plant pigments from the oil, they are trace substances that are not detectable by FT-IR.

As shown in the inserted graph in Figure 6, the relationship between the 1713 cm^{-1} band and the FFA determination is strikingly linear. A classical univariate linear regression model results in an RMSECV of 0.12 and a correlation coefficient, R^2, of 0.996—slightly better than the multivariate PLS model. In light of such an exceptionally good relationship, one may question the relevance of applying multivariate algorithms. However, for most practical purposes, multivariate PLS models will behave more robustly and facilitate outlier detection.

In the FT-IR region, principal variable selection is important because we can usually interpret the spectral elements on a group frequency basis. Table 4 lists the result of principal variable selection based on the FT-IR ensemble in the form of the three most influential spectral elements and the corresponding best MLR models. As apparent from the table, all models use the carboxylic carbonyl stretch from FFA as their main principal variable. The strongly absorbing fatty acid ester carbonyl stretch at 1745 cm^{-1} is in fact only used in the TG model (and in the weaker IV and vita-E models). The MLR results (Table 4) showed that the MLR models based on few optimal variables are as good as the full spectral PLS models listed in Table 3. When considering the principal variables, a new spectral element appears at approximately 1732 cm^{-1} in between the two main carbonyl stretches. This band covaries almost perfectly with the acid stretch at 1713 cm^{-1}, which can perhaps be assigned to a fraction of the FFA that is unassociated (not dimerized). The two-component principal variable/MLR model for FFA has improved RMSECV slightly when compared to the univariate model described above.

TABLE 4
The Three Most Influencial Wavenumbers in the FT-IR Models as Determined by the Principal Variable Method and the Corresponding Best Cross-Validated MLR Models[a]

	Principal variable			MLR		
Model	σ_1	σ_2	σ_3	Prin. var.	RMSECV	R^2
DAYS	1713	2919	1750	3	2.15	0.86
VISC	1713	1559	2914	1	2.45	0.82
DPTG	1714	1731	1745	2	0.47	0.96
TG	1713	1745	1734	3	0.51	1.00
DG	1713	1559	2915	2	0.31	1.00
MG	1713	1733	1745	2	0.04	0.99
FFA	1713	1736	1745	2	0.10	1.00
OT	1713	1732	2918	3	0.27	0.80
IV	1713	1729	1744	3	4.78	0.86
Vita-E	1714	1732	1745	3	30.58	0.90

[a]Wavenumbers are in reciprocal centimeters. The sequence σ_1, σ_2, σ_3 indicates decreasing influence. MLR, multiple linear regression; Prin. var., principal variable. See Tables 1 and 2 for other abbreviations.

NIR FT-Raman spectroscopy. The development of FT interferometers (39) and NIR lasers for use in Raman spectroscopy has suddenly made Raman spectroscopy an interesting and promising technique for use in the agricultural and food sciences. NIR FT-Raman has proved useful in determining total level of unsaturation, *cis*/*trans* isomer ratios, and the total number of double bonds in hydrocarbon chains (40,41).

The Raman-shifted spectra of the 20 oil samples are shown in Figure 7A. The spectra display almost the same details, except for an increasing scatter toward low wavenumbers as a function of increasing frying time. In the mid-wavenumber region, we find two peaks at 1302 and 1440 cm^{-1}, corresponding to polymethylene twisting and scissoring, respectively. Carbon-carbon double-bond stretching is found as a sharp and relatively strong peak at 1656 cm^{-1}, characteristic of *cis* olefins. In the carbonyl region, we find only a broad and weak peak, centered around 1748 cm^{-1}, corresponding to the ester C=O stretch. In the aliphatic CH stretching region, the two main peaks at 2852 and 2925 cm^{-1} correspond to polymethylene symmetric and asymmetric CH stretchings, respectively. The peak at 3009 cm^{-1} is due to olefinic =C–H strechings in *cis* configurations.

The PCA score plot in Figure 7B displays a more distorted sample trend than for the fluorescence and NIR/VIS spectral ensembles, probably due to the inherent lower signal-to-noise ratio of the Raman scatter. What is perhaps more interesting is that the gap between samples 11 and 12 is absent and that there is considerably more systematic variation in the samples from the last 2 wk.

The performance of the full-spectral PLS models, based on the Raman spectra (Raman shift 300 to 3300 cm^{-1}), is listed in Table 3. To our surprise, the PLS model for frying time (DAYS) was superior to the other spectral ensembles. Analysis showed that the exceptionally good PLS model was due to increasing Raman scatter at low wavenumbers in the samples (see covarygram in Fig. 8). Raman scatter originates from either fluorescence phenomena and/or from increasing amounts of suspended materials in the frying oils. However, the scatter more likely originates from fluorescence phenomena because the particle scatter present in the IR region was highly correlated to DPTG, but not to DAYS, and because the Rayleigh scatter was less, and negatively, correlated to DAYS. The predicted vs. measured plot of the PLS model to DAYS in Figure 9B indicates that the reason for the good correlation is a tendency to group the samples into scatter groups, including the relatively large spread in the samples from the last 2 wk. For comparison, the corresponding plot based on the NIR/VIS spectra (Fig. 9A) displays more typical spectral

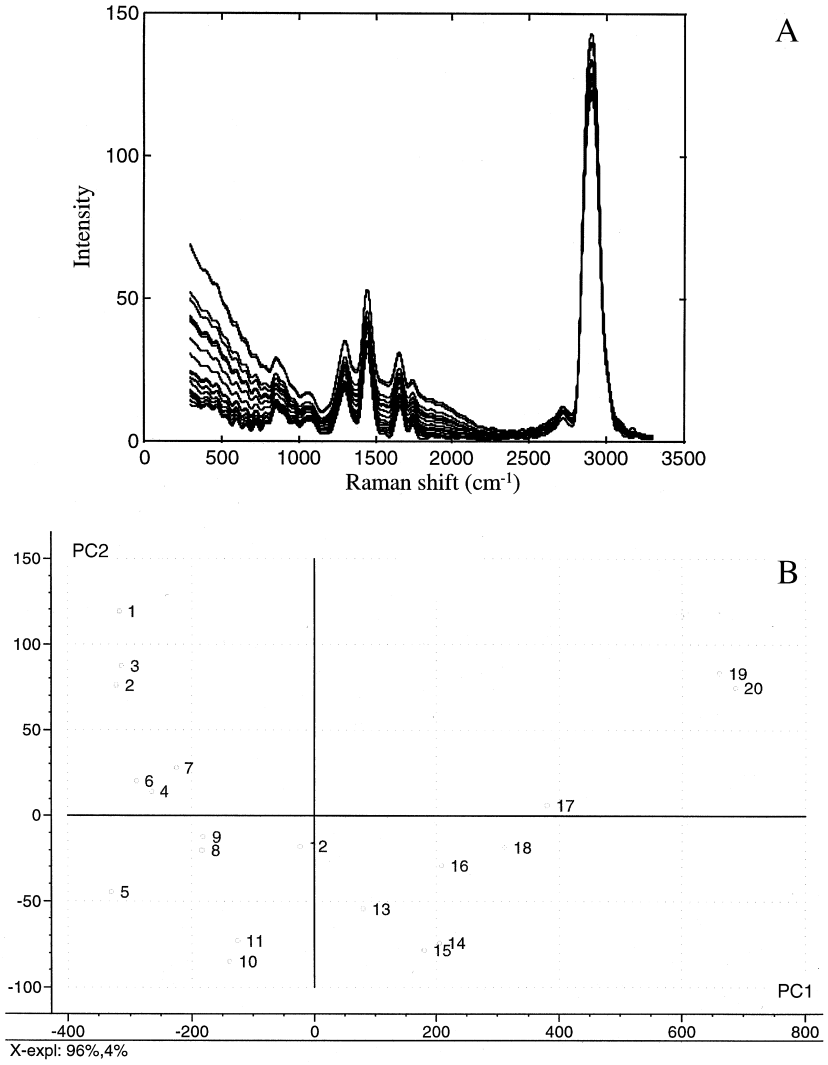

FIG. 7. (A) Near-infrared (NIR) FT-Raman spectra (at 64 cm^{-1} resolution) of the 20 oil samples. (B) Score plot from PCA on NIR FT-Raman data as a function of the two first PC, describing 96 and 4% of the spectral variation, respectively. See Figures 1 and 5 for other abbreviations.

behavior with a clear nonlinear tendency, and the samples from the last 2 wk clustered in a swarm, resulting in poor correlation.

The remaining Raman PLS models were inferior to the other spectral ensembles except for the OT model, which is apparently also correlated to the Raman scatter. Ozaki *et al.* (41) found a linear correlation between IV and the intensity ratio I_{1658}/I_{1443}. By performing a logarithmic pretransformation prior to the regression analysis, to make the relative intensities additive, we found a one-PC model for IV (RMSECV = 4.5) that was slightly better than models based on the raw and derivative spectra but still inferior to the PLS models based on the NIR/VIS and fluorescence spectra. Finally, all PLS models based on Raman spectra were slightly better when recorded at low resolution (64 cm^{-1}) than when recorded at high resolution (4 cm^{-1}).

The present investigation has demonstrated the possibilities of using different spectroscopic sensors, along with multivariate chemometric methods, for monitoring the physicochemical changes that occur in oil during an industrial frying operation. It appears that FT-IR with the ATR sampling technique was a most direct and accurate method of monitoring the gross changes in the frying oil, as reflected by the thermal decomposition of TG into FFA. NIR/VIS and fluorescence spectroscopy perform almost equally well *via* indirect correlations from chromophores and fluorophores, respectively. The investigation has demonstrated that it is possible, without significant loss of accuracy, to replace titration and chromatographic procedures with fast noninvasive spectroscopic methods. Finally, spectroscopy in combination with multivariate projection tools has great potential to be used on-line to monitor and optimize the unit operation of deep frying.

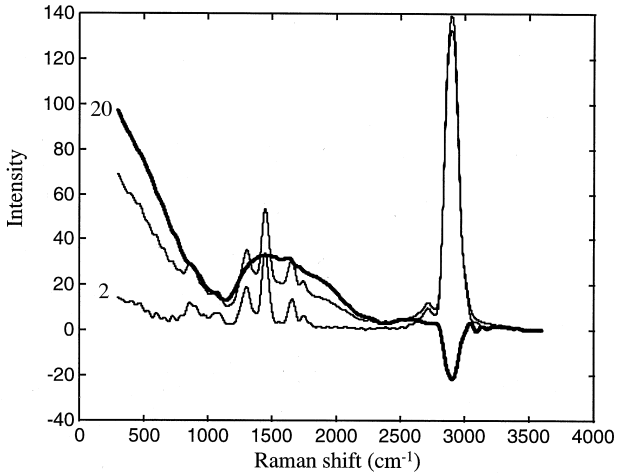

FIG. 8. Covarygram (thick line) to show the covariance between the Raman spectra (Raman-shifted) and DAYS. Thin lines depict the spectra of samples 2 and 20. See Figure 1 for abbreviation.

ACKNOWLEDGMENTS

This investigation was sponsored by funds to Professor Lars Munck from the Danish Research Councils 13-4804-1 (agriculture) and from the Department of Education donated to the Danish Centre for Advanced Food Studies (LMC). We are indebted to Jeanette Saabye of Daloon A/S for collecting the oil samples and making them available to us. I also thank Associate Professor Lars Nørgaard for helpful discussions concerning the chemometric aspects of this study, Professor Lars Munck for helpful comments on the manuscript, engineer John Hørlyck and lab technician Peter K. Henriksen for helping in the collection of the spectral data, Ph.D. student Claus Jensen for measuring the vita-E data, and student Jette Nysom for measuring the OT, IV, and PV data.

REFERENCES

1. Artman, N.P., The Chemical and Biological Properties of Heated and Oxidized Fats, *Adv. Lipid Res. 7*:245–330 (1969).
2. Fritch, C.W., Measurements of Frying-Fat Deterioration: A Brief Review, *J. Am. Oil Chem. Soc. 58*:272–274 (1981).

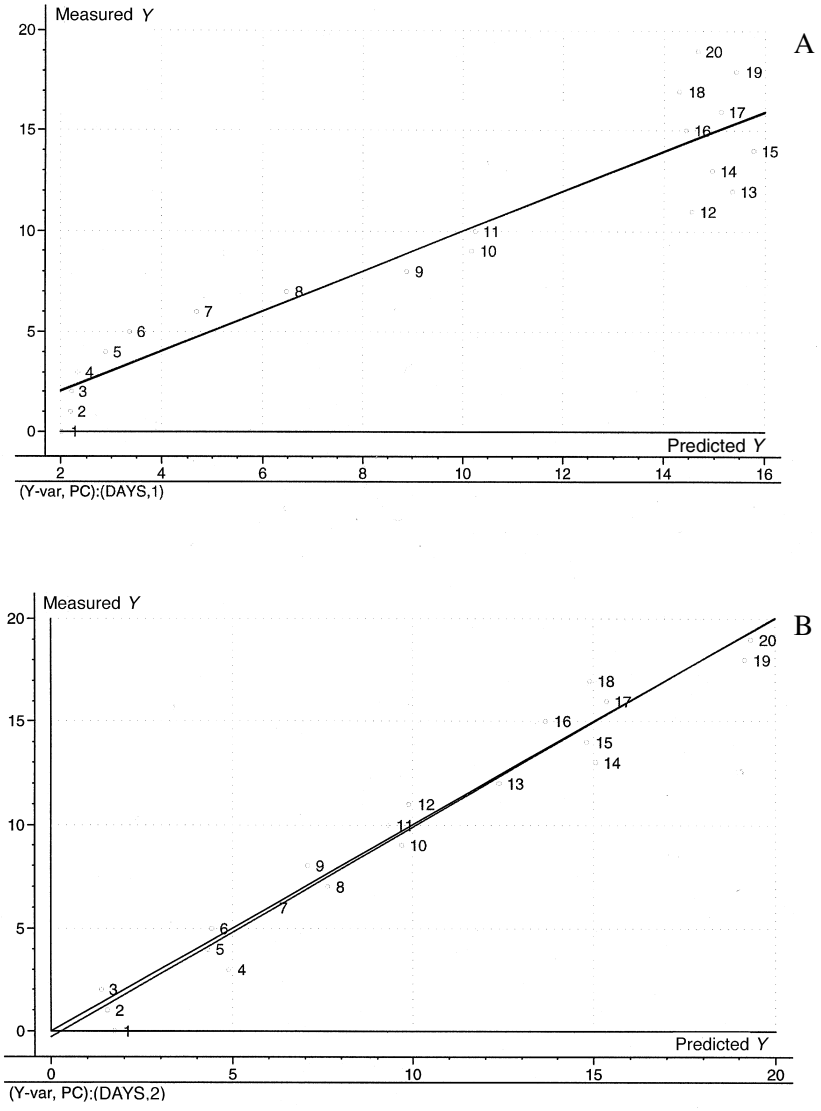

FIG. 9. (A) Predicted vs. measured plot of the one-PC partial least squares (PLS) model to DAYS based on the NIR/VIS spectral ensemble. (B) Predicted vs. measured plot of the two-PC PLS model to DAYS using the Raman spectral ensemble (Raman-shifted) of the 20 oil samples. See Figures 1 and 4 for other abbreviations.

3. Billek, G., Heated Oils—Chemistry and Nutritional Aspects, *Nutr. Metab. 24*:200–210 (1980).
4. Chang, S.S., R.J. Peterson, and C.-T. Ho, Chemical Reactions Involved in the Deep-Fat Frying of Foods, *J. Am. Oil Chem. Soc. 55*:718–727 (1978).
5. Firestone, D., R.F. Stier, and M.M. Blumental, Regulation of Frying Fats and Oils, *Food Technol. 2*:90–94 (1991).
6. Wu, P., and W.W. Nawar, A Technique for Monitoring the Quality of Used Frying Oils, *J. Am. Oil Chem. Soc. 63*:1363–1367 (1986).
7. Li-Chan, E., Developments in the Detection of Adulteration of Olive Oil, *Trends Food Sci. Technol. 5*:3–11 (1994).
8. Lai, Y.W., E.K. Kemsley, and R.H. Wilson, Quantitative Analysis of Potential Adulterants of Extra-Virgin Olive Oil Using Infrared Spectroscopy, *Food Chem. 53*:95–98 (1995).
9. IUPAC, *Standard Methods for the Analysis of Oils, Fats and Derivatives,* 7th revised and enlarged edn., 1982.
10. *Official Methods and Recommended Practices of the American Oil Chemists' Society*, 4th edn., edited by D. Firestone, American Oil Chemists' Society, Champaign, 1989.
11. Podda, M., C. Weber, M.G. Traber, and L. Packer, Simultaneous Determination of Tissue Tocopherols, Tocotrienols, Ubiquinols, and Ubiquinones, *J. Lipid Res. 37*:893–901 (1996).
12. Wold, S., K. Esbensen, and P. Geladi, Principal Components Analysis, *Chemometr. Intell. Lab. Syst. 2*:37–52 (1987).
13. Engelsen, S.B., and L. Nørgaard, Comparative Vibrational Spectroscopy for Determination of Quality Parameters in Amidated Pectins as Evaluated by Chemometrics, *Carbohydr. Polym. 30*:9–24 (1996).
14. Geladi, P., and B.R. Kowalski, Partial Least-Squares Regression: A Tutorial, *Anal. Chim. Acta 185*:1–17 (1987).
15. Martens, H., and S.A. Jensen, Partial Least Squares Regression: A New Two-Stage NIR Calibration Method, in *Progress in Cereal Chemistry and Technology*, edited by J. Holas and J. Kratochvil, Elsevier, Amsterdam, Vol. 5a, 1983, pp. 607–647.
16. Höskuldsson, A., The H-Principle: New Ideas, Algorithms and Methods in Applied Mathematics, *Chemometr. Intell. Lab. Syst. 23*:1–28 (1994).
17. Wold, S., Cross-Validatory Estimation of the Number of Components in Factor and Principal Components Models, *Technometrics 20*:397–405 (1978).
18. Firestone, D., Worldwide Regulation of Frying Fats and Oils, *INFORM 4*:1366–1371 (1993).
19. Landers, R.E., and D.M. Rathmann, Vegetable Oils: Effects of Processing, Storage and Use on Nutritional Value, *J. Am. Oil Chem. Soc. 58*:255–259 (1981).
20. Stevenson, S.G., M. Vaisey-Genser, and N.A.M. Eskin, Quality Control in the Use of Deep-Frying Oils, *Ibid. 61*:1102–1108 (1984).
21. Billek, G., G. Guhr, and J. Waibel, Quality Assessment of Used Frying Fats: A Comparison of Four Methods, *Ibid. 55*:728–733 (1978).
22. IUPAC, Standard Methods for the Analysis of Oils, Fats and Derivatives, 6th edn., 1st Supplement part 4, *Pure Appl. Chem. 54*:233–245 (1982).
23. Paradis, A.J., and W.W. Nawar, A Gas-Chromatographic Method for the Assessment of Used Frying Oils: Comparison with Other Methods, *J. Am. Oil Chem. Soc. 58*:635–638 (1981).
24. Blumental, M.M., A New Look at the Chemistry and Physics of Deep-Fat Frying, *Food Technol. 2*:68–71 (1991).
25. Brooks, D.D., Some Perspectives on Deep-Fat Frying, *INFORM 2*:1091–1095 (1991).
26. Augustin, M.A., and S.K. Berry, Efficacy of the Antioxidants BHA and BHT in Palm Olein During Heating and Frying, *J. Am. Oil Chem. Soc. 60*:1520–1523 (1983).
27. Perkins, E.G., Formation of Nonvolatile Decomposition Products in Heated Fats and Oils, *Food Technol. 21*:611–616 (1967).
28. Melton, S.L., S. Jafar, D. Sykes, and M.K. Trigano, Review of Stability Measurements for Frying Oils and Fried-Food Flavor, *J. Am. Oil Chem. Soc. 71*:1301–1308 (1994).
29. Cathcart, R., E. Schwiers, and B.N. Ames, Detection of Picomole Levels of Hydroperoxides Using a Fluorescent Dichlorofluorescein Assay, *Anal. Biochem. 134*:111–116 (1983).
30. Hølmer, G., Methods for Detection of Oxidative Changes in Lipids, LIPIDFORUM, *Proceedings of the 17th Nordic Lipid Symposium*, Imatra, Finland, 1993, pp. 114–137.
31. Duggan, D.E., R.L. Bowman, B.B. Brodie, and S. Udenfriend, A Spectrophotofluorometric Study of Compounds of Biological Interest, *Arch. Biochem. Biophys. 68*:1–14 (1957).
32. Kourti, T., and J.F. MacGregor, Process Analysis, Monitoring and Diagnosis, Using Multivariate Projection Methods, *Chemometr. Intell. Lab. Syst. 28*:3–21 (1995).
33. Holman, R.T., and P.R. Edmondson, Near-Infrared Spectra of Fatty Acids and Some Related Substances, *Anal. Chem. 28*:1533–1538 (1956).
34. Sato, T., S. Kawano, and M. Iwamoto, Near-Infrared Spectral Patterns of Fatty Acid Analysis from Fats and Oils, *J. Am. Oil Chem. Soc. 68*:827–833 (1991).
35. van de Voort, F.R., J. Sedman, G. Emo, and A.A. Ismail, Rapid and Direct Iodine Value and Saponification Number Determinations of Fats and Oils by Attenuated Total Reflectance/Fourier Transform Infrared Spectroscopy, *Ibid. 69*:1118–1123 (1992).
36. Ismail, A.A., F.R. van de Voort, G. Emo, and J. Sedman, Rapid Quantitative Determination of Free Fatty Acids in Fats and Oils by Fourier Transform Infrared Spectroscopy, *Ibid. 70*:335–341 (1993).
37. van de Voort, F.R., A.A. Ismail, J. Sedman, and G. Emo, Monitoring the Oxidation of Edible Oils by Fourier Transform Infrared Spectroscopy, *Ibid. 71*:243–253 (1994).
38. van de Voort, F.R., A.A. Ismail, J. Sedman, J. Dubois, and T. Nicodemo, The Determination of Peroxide Value by Fourier Transform Infrared Spectroscopy, *Ibid. 71*:921–926 (1994).
39. Hirschefeld, T., and B. Chase, FT-Raman Spectroscopy: Development and Justification, *Appl. Spectrosc. 40*:133–137 (1986).
40. Sadeghi-Jorabchi, H., R.H. Wilson, P.S. Belton, J.D. Edwards-Webb, and D.T. Coxon, Quantitative Analysis of Oils and Fats by Fourier Transform Raman Spectroscopy, *Spectrochim. Acta 47A*:1449–1458 (1991).
41. Ozaki, Y., R. Cho, K. Ikegaya, S. Muraishi, and K. Kawauchi, Potential of Near-Infrared Fourier Transform Raman Spectroscopy in Food Analysis, *Appl. Spectrosc. 46*:1503–1507 (1992).

[Received September 27, 1996; accepted July 23, 1997]